Title
Neomorphic effects of recurrent somatic mutations in Yin Yang 1 in insulin-producing adenomas.

Authors
Cromer, M
Cromer, M
Choi, Murim
et al.

Peer reviewed

Neomorphic effects of recurrent somatic mutations in *Yin Yang 1* in insulin-producing adenomas

M. Kyle Cromer[a,b], Murim Choi[a,b], Carol Nelson-Williams[a,b], Annabelle L. Fonseca[c,d,e], John W. Kunstman[c,d,e], Reju M. Korah[c,d,e], John D. Overton[a,f], Shrikant Mane[a,f], Barton Kenney[g], Carl D. Malchoff[h,i], Peter Stalberg[j], Göran Akerström[j], Gunnar Westin[j], Per Hellman[j], Tobias Carling[c,d,e], Peyman Björklund[j], and Richard P. Lifton[a,b,f,k,1]

Departments of [a]Genetics, [c]Surgery, [g]Pathology, and [k]Internal Medicine, [b]Howard Hughes Medical Institute, [d]Yale Endocrine Neoplasia Laboratory, [e]Yale Cancer Center, and [f]Yale Center for Genome Analysis, Yale University School of Medicine, New Haven, CT 06510; [h]Division of Endocrinology and [i]Neag Cancer Center, University of Connecticut Health Center, Farmington, CT 06030; and [j]Department of Surgical Sciences, Uppsala University, Uppsala, Sweden 751 05

Insulinomas are pancreatic islet tumors that inappropriately secrete insulin, producing hypoglycemia. Exome and targeted sequencing revealed that 14 of 43 insulinomas harbored the identical somatic mutation in the DNA-binding zinc finger of the transcription factor Yin Yang 1 (YY1). Chromatin immunoprecipitation sequencing (ChIP-Seq) showed that this T372R substitution changes the DNA motif bound by YY1. Global analysis of gene expression demonstrated distinct clustering of tumors with and without *YY1^T372R* mutations. Genes showing large increases in expression in YY1^T372R tumors included *ADCY1* (an adenylyl cyclase) and *CACNA2D2* (a Ca^2+ channel); both are expressed at very low levels in normal β-cells and show mutation-specific YY1 binding sites. Both gene products are involved in key pathways regulating insulin secretion. Expression of these genes in rat INS-1 cells demonstrated markedly increased insulin secretion. These findings indicate that YY1^T372R mutations are neomorphic, resulting in constitutive activation of cAMP and Ca^2+ signaling pathways involved in insulin secretion.

exome sequencing | insulinoma | YY1 | cAMP | adenylyl cyclase

Plasma glucose levels are normally tightly regulated by insulin secreted from β-cells of the pancreatic islets of Langerhans. Insufficient insulin secretion results in high blood glucose and diabetes mellitus. Conversely, too much insulin secretion results in hypoglycemia, with neuromuscular complications progressing from confusion and weakness to coma and seizures with worsening hypoglycemia. Insulin-producing tumors, nearly always of pancreatic origin, are the most common cause of fasting hypoglycemia in the absence of exogenous insulin administration (1). About 90% of these tumors are small, benign adenomas with little malignant potential, and are cured by surgery (2).

The mechanisms linking tumor growth and autonomous insulin secretion have been obscure. Insulin secretion is normally stimulated by increased intracellular Ca^2+ (*SI Appendix*, Fig. S1). Quiescent cells maintain a highly negative resting potential owing to the constitutively open inwardly-rectifying K^+ channel, subfamily J, member 11 (KCNJ11) (*SI Appendix*, Fig. S1A). Metabolism of glucose in β-cells results in increased intracellular ATP, which inactivates KCNJ11, resulting in cell depolarization (3), activation of voltage-gated Ca^2+ channels, and increased intracellular Ca^2+, which promotes insulin secretion via fusion of insulin-containing vesicles with the plasma membrane (4).

In addition to this classical pathway, nutrients in the gut cause intestinal epithelia to release the peptide hormone glucagon-like peptide 1 (GLP-1), an agonist for glucagon-like peptide 1 receptor (GLP1R), a G protein-coupled receptor (GPCR) on pancreatic β-cells (*SI Appendix*, Fig. S1B) (5, 6). GLP1R signaling via its Gα subunit increases cAMP formation through activation of adenylyl cyclase 6 (*ADCY6*) and *ADCY8* (7, 8). cAMP binds to cAMP-GEF, which potentiates insulin secretion by causing transient spikes of intracellular Ca^2+ (9); other mechanisms may contribute as well (6). This cAMP-dependent effect is synergistic with voltage-dependent activation of Ca^2+ channels and

provides the basis for the clinical efficacy of GLP-1 and inhibitors of dipeptidyl peptidase 4, which normally degrades GLP-1; these drugs increase glucose-dependent insulin secretion and lower blood glucose (10).

Sustained elevations in both intracellular Ca^2+ and GLP-1 signaling are known to also promote proliferation of β-cells (11, 12). This observation raises the possibility that single mutations that increase activity of one or both of these axes might explain both the cell proliferation and autonomous insulin secretion seen in insulinomas. Recent studies of aldosterone-producing adenomas (APAs) (13–15) and adrenal cortisol-producing adenomas (16, 17) support this possibility. Both tumors feature very few somatic mutations. In APAs, recurrent somatic mutations in the gene encoding the inwardly-rectifying K^+ channel, subfamily J, member 5 (*KCNJ5*) in adrenal glomerulosa cells allow aberrant Na^+ conductance, resulting in membrane depolarization, activation of voltage-gated Ca^2+ channels, and Ca^2+ entry, the signal for aldosterone production and cell proliferation. The same pathway is activated by gain-of-function mutations in the gene encoding the alpha 1D subunit of the voltage-dependent, L-type Ca^2+ channel (*CACNA1D*). That these single mutations are sufficient for tumor production comes from rare syndromes featuring constitutive hormone production with adrenal hyperplasia in patients with the same mutations occurring in the germ line (13, 14). Similarly, somatic mutations that increase activity of the cAMP signaling pathway in adrenal fasciculata

Significance

The identical recurrent somatic heterozygous missense mutation in the DNA-binding domain of transcription factor YY1 is found in a third of insulin-secreting pancreatic tumors. This mutation alters sites involved in DNA contact and changes the DNA sequence motif that is bound, resulting in significant alteration of gene expression. Among genes showing markedly increased expression are two, an adenylyl cyclase (*ADCY1*) and a Ca^2+ channel (*CACNA2D2*), that are involved in cAMP and Ca^2+ signaling, processes known to play a role in insulin secretion. Expression of these genes in a pancreatic β-cell line causes increased insulin release. These findings provide evidence for neomorphic effects of this mutation, and demonstrate a role for altered transcription factor specificity in neoplasia.

are frequently found in adrenal cortisol-producing adenomas (16, 17).

Prior studies of insulinomas have demonstrated that homozygous loss of the multiple endocrine neoplasia 1 gene (*MEN1*) via inherited and/or acquired mutations plays a role in the pathogenesis of several endocrine tumors, including a small fraction of insulinomas (18, 19). Recently, exome sequencing of insulinomas identified a recurrent somatic missense mutation in the transcription factor *YY1* in nearly one-third of insulinomas (20). This mutation, *YY1^{T372R}*, occurs in the completely conserved third zinc finger domain and substitutes arginine for threonine between flanking amino acids that make direct contact with DNA and define the DNA-binding motif of YY1. Via its ability to bind DNA, RNA, and protein cofactors, YY1 can induce or repress expression of many genes, frequently with opposite effects on the same gene in different cell types (21–23). The mechanism by which the *YY1^{T372R}* mutation contributes to insulinoma pathogenesis remains to be elucidated. It has been suggested that these mutations may contribute to disease by increased transcriptional activation of normal target genes (20); however, the possibility of neomorphic effects has not been explored.

Results

Exome Sequencing of Insulinomas.
We studied a cohort of 33 patients with benign insulinomas. None had a family history of insulinoma or multiple endocrine neoplasia type 1. All presented with signs and symptoms of hypoglycemia. Measurement of fasting blood glucose and insulin revealed significant hypoglycemia with inappropriately elevated insulin levels (*SI Appendix*, Table S1). Imaging studies revealed pancreatic tumors, which were surgically removed, revealing benign islet cell tumors (*SI Appendix*, Fig. S2). In all cases, surgery corrected the hypoglycemia. We studied 10 additional patients with malignant insulinomas (*SI Appendix*, Table S1).

DNA from seven benign insulinomas and matched blood samples was subjected to exome sequencing (18, 19). Tumor exomes were sequenced to a median coverage of 287 independent reads per targeted base, with 96% of all targeted bases read at least 20 times (*SI Appendix*, Table S2).

Segments with somatic loss of heterozygosity (LOH) were identified by differences in minor allele frequencies of heterozygous SNPs in tumor and matched normal DNA (*SI Appendix*, Fig. S3). Putative somatic single-base substitutions or small insertion–deletion mutations were identified from significant differences in read counts between tumor and germ-line DNA. All such somatic mutations were confirmed by direct Sanger sequencing of PCR amplicons. From these data, the mean purity of tumor cells in each sample was estimated to be 55% (range 39–73%) (*SI Appendix*, Table S2).

Consistent with experience in other benign endocrine-producing tumors, each insulinoma had a very small number of somatic mutations. There was a mean of 1.4 segments of LOH per tumor, with chromosomes 11 and 16 showing LOH in two samples each (*SI Appendix*, Fig. S3 and Table S3). There was a mean of only 3.7 protein-altering somatic mutations per tumor (range 0–7) (*SI Appendix*, Table S3) and an overall somatic mutation rate in the targeted exome of 1×10^{-7}.

One tumor harbored a somatic missense mutation in *MEN1*, the gene responsible for multiple endocrine neoplasia type 1 and a known contributor to pancreatic islet tumors (24). The mutation identified, R457P, occurs at a highly conserved position in the encoded protein and lies in a segment of somatic LOH in the tumor, consistent with somatic loss of both *MEN1* alleles. Another tumor displayed a heterozygous somatic mutation in *SMARCA4*, a member of the SWI/SNF chromatin remodeling family that has recently been implicated in tumorigenesis in a variety of tissue types (25). This mutation substituted serine for proline at residue 930, which is a highly conserved position in the ATPase domain (*SI Appendix*, Table S3).
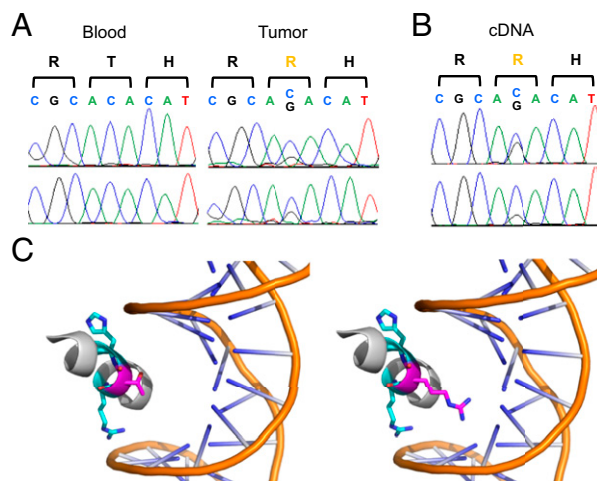
Recurrent Somatic *YY1^{T372R}* Mutation.
Two of the seven insulinomas harbored the identical somatic missense mutation previously reported, substituting arginine for threonine at amino acid 372 in the transcription factor YY1 (YY1^{T372R}; Fig. 1*A*) (20). In both cases, the mutation was not in a segment of LOH, and both exome read counts and Sanger sequencing were consistent with the mutation being heterozygous. Each tumor had only four other protein-altering somatic mutations, none of which were in notable candidate genes or mutated in more than one tumor (*SI Appendix*, Table S3). *YY1^{T372R}* is expressed in RNA from tumors harboring this mutation (Fig. 1*B*).

Sequencing of *YY1* in the additional 26 benign insulinomas identified another 9 tumors with the identical somatic *YY1^{T372R}* mutation (*SI Appendix*, Fig. S4), and no other *YY1* mutations were found. Similarly, *YY1^{T372R}* was found in 3 of 10 malignant insulinomas. This frequency of the *YY1^{T372R}* mutation in 14/43 insulinomas (11/33 benign, 3/10 malignant) is similar to the results recently reported (20).

We found no significant difference between *YY1^{T372R}* and *YY1^{WT}* tumors in age at tumor resection, tumor size, sex ratio, fasting glucose, or insulin level.

Wild-type YY1 (YY1^{WT}), which can activate or repress gene expression (21), binds DNA at a consensus motif containing 5′-GCCATNTT-3′ (26). In the crystal structure of YY1 bound to DNA, threonine 372 lies between the two amino acids in the third zinc finger that directly contact DNA and that determine the recognition motif (Fig. 1*C*) (27). This entire zinc finger domain is completely conserved from fruit flies to humans (26), supporting the functional significance of the T372R mutation. The short T372 side chain projects toward but does not contact DNA (Fig. 1*C*).

YY1^{T372R} Mutation Alters the YY1 DNA-Binding Motif.
It seems highly likely that the longer and positively charged side chain introduced by the T372R mutation alters the DNA recognition motif of YY1, suggesting neomorphic effects. To address this possibility, we prepared Myc-tagged constructs containing either *YY1^{WT}* or *YY1^{T372R}* and expressed these in HEK293T cells; YY1^{WT} and YY1^{T372R} were

Fig. 1. Recurrent somatic mutation in *YY1* in insulinomas. (*A*) Sanger sequencing of matched germ-line and tumor genomic DNA of *YY1* codons 371–373. Forward and reverse sequences are shown, confirming the T372R mutation identified by exome sequencing. (*B*) Sanger sequencing of tumor cDNA of *YY1* codons 371–373. Forward and reverse sequences are shown, demonstrating expression of the *YY1^{T372R}* mutant allele. (*C*) Representation of the crystal structure of the third YY1 zinc finger domain bound to DNA at the wild-type binding sequence. The threonine at residue 372 (magenta) lies between an arginine at residue 371 and a histidine at residue 373 (both cyan), which directly contact DNA at the recognition motif. Projection of the YY1^{T372R} side chain is shown (*Right*).

expressed at virtually identical levels (*SI Appendix*, Fig. S5). DNA was cross-linked to chromatin with formaldehyde, and immuno-precipitation was performed with an anti-Myc antibody. Following immunoprecipitation, the cross-links were reversed and the liberated DNA was subjected to sequencing on the Illumina HiSeq platform, with a mean of 3 Gb of DNA sequence produced per sample. Biological replicates were analyzed from cells expressing either $YY1^{WT}$ or $YY1^{T372R}$. Sequences enriched by immunoprecipitation were identified (28, 29).

The only motif significantly enriched by ChIP with $YY1^{WT}$ was 5′-GCCATNTT-3′, virtually identical to the published recognition sequence (Fig. 2*A*) (26). Using the FIMO program (30) to identify this motif in ChIP peaks revealed approximately fourfold enrichment of this motif compared with its occurrence in random human genome sequences, with a mean of 0.45 instances per trimmed ChIP-seq (sequencing) peak (Table 1). In contrast, ChIP-seq with $YY1^{T372R}$ showed strong enrichment of a shorter motif, 5′-CCATC-3′ (Fig. 2*A*). This motif was enriched more than 80-fold among ChIP peaks, with a mean of 7.7 instances of the motif per trimmed ChIP peak, and bound more sites than $YY1^{WT}$ (Table 1). This 5′-CCATC-3′ motif retains a core 5′-CCAT-3′ sequence found in the $YY1^{WT}$ motif, adds specificity for cytosine at the 3′ end of this sequence where $YY1^{WT}$ has no strong preference, and drops sequence requirements both 5′ and 3′ to these positions. Not surprisingly, therefore, $YY1^{T372R}$ ChIPs most (80.5%) of the $YY1^{WT}$ binding sites (Table 1). In conjunction with the genetic data, we anticipate that this aberrant binding will activate or repress genes not normally regulated by $YY1^{WT}$ and that such alterations may contribute to or cause insulinomas.

Altered Gene Expression in Tumors with $YY1^{T372R}$. We next analyzed gene expression in five insulinomas with $YY1^{T372R}$ and six insulinomas without this mutation on the Affymetrix GeneChip Human Gene 1.0 ST Array platform. Unsupervised clustering by principal component analysis (PCA) identified two distinct groups of tumors that corresponded to insulinomas with and without $YY1^{T372R}$ (Fig. 2*B*). The Euclidean distances separating pairs of tumors with the $YY1^{T372R}$ mutation were significantly smaller than distances between $YY1^{T372R}$ and $YY1^{WT}$ pairs ($P < 7 \times 10^{-6}$). The first three principal components collectively accounted for 48% of the total variance in expression among all of the tumors (PC1, PC2, and PC3 account for 25%, 12%, and 11% of the variance, respectively).

We compared the expression of 519 genes reported to be regulated by $YY1^{WT}$ in tumors with $YY1^{WT}$ and $YY1^{T372R}$ (31). We found no significant difference, with a median 15% reduction in expression in YY1 targets in mutant tumors compared

Fig. 2. Altered $YY1^{T372R}$ DNA-binding motif imparts a unique expression signature. (*A*) Motifs enriched by ChIP-seq following expression of $YY1^{WT}$ and $YY1^{T372R}$ in HEK293T cells compared with the published $YY1^{WT}$ motif. Sites at which R371 and H373 of $YY1^{WT}$ contact the DNA backbone between bases of the recognition motif are indicated by blue and orange arrows, respectively. (*B*) Expression profiles of $YY1^{T372R}$-harboring tumors (red) are distinct from those with $YY1^{WT}$ (blue). Expression of all probes on the microarray for each tumor was used as input for unsupervised clustering by PCA.

Table 1. Motif enrichment in ChIP-seq peaks

Sample	No. of peaks	Mean $YY1^{WT}$ motifs per peak	Mean $YY1^{T372R}$ motifs per peak
$YY1^{WT}$ IP	6,514	0.45	0.09
$YY1^{T372R}$ IP	16,614	0.36	7.68
Random sequence	—	0.11	0.09

Peaks that reproduced in biological replicates are reported. The top 10% of peaks (by enrichment score) were used as input to calculate the mean number of motifs in the 400 bp flanking the summit of each peak.
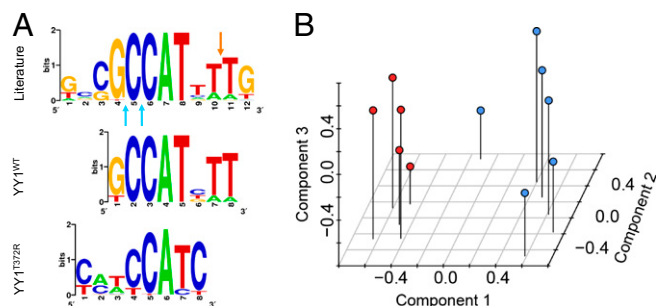
with wild type. Although $YY1^{WT}$ overexpression has been shown to increase the expression of mitochondrial genes (32), we did not find any nuclear-encoded mitochondrial genes among the differentially expressed gene set (*SI Appendix*, Table S4), and no enrichment of mitochondrial genes among those showing significantly altered expression (using $P < 0.01$, 50 mitochondrial genes surpassed this threshold, with 51 expected by chance alone). In addition, we found no significant change in expression between mitochondrial and nonmitochondrial genes in tumors with or without the $YY1$ mutation ($P = 0.89$). This lends further support to a neomorphic effect (a new activity not present in the wild-type gene product) for $YY1^{T372R}$ rather than a simple gain-of-function (increased level of normal gene product activity) mechanism as previously suggested (20).

Increased Expression of *ADCY1* and *CACNA2D2* in $YY1^{T372R}$ Tumors. To identify differentially regulated genes potentially driving insulinoma pathogenesis in $YY1^{T372R}$ tumors, we directly compared the expression of each gene in $YY1^{T372R}$ and $YY1^{WT}$ tumors. This revealed 149 genes with at least a 10-fold and significant ($P < 0.01$) difference in expression between the two groups (*SI Appendix*, Table S4). Only one of these genes, *GIPC2*, is a reported $YY1^{WT}$ target, and none are known mitochondrial genes (32).
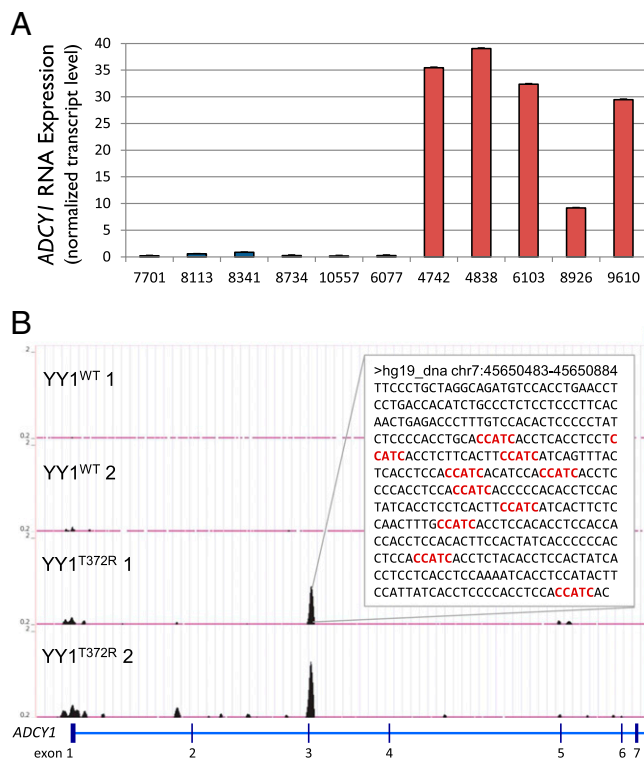
From this set, we identified candidates for follow-up that displayed strong differential expression that have plausible roles in insulin secretion based on known physiology. One of the strongest candidates was adenylyl cyclase 1 (ADCY1), which catalyzes the synthesis of cAMP. *ADCY1* is the only neuro-specific adenylyl cyclase (33), and shows no expression above background in normal pancreatic islets (34–36) and tumors with $YY1^{WT}$ (Fig. 3*A*). In tumors with $YY1^{T372R}$, however, *ADCY1* expression is increased more than 90-fold above background, placing its absolute expression level among the top 1% of all genes in these tumors. All 20 probes for *ADCY1* showed increased expression, and the difference in expression was highly significant ($P < 4 \times 10^{-6}$) (*SI Appendix*, Table S4).

A second gene of interest was *CACNA2D2*, which encodes the alpha-2-delta-2 auxiliary (pore-forming) subunit of a high voltage-gated Ca^{2+} channel. *CACNA2D2* expression was near background level in all but one $YY1^{WT}$ tumor but has 13-fold increased expression in $YY1^{T372R}$ tumors, with expression among the top 5% of all genes in these tumors (*SI Appendix*, Fig. S6 and Table S4). Variation in expression of both *ADCY1* and *CACNA2D2* contributes to explaining the variance in PC1, ranking in the top 0.1% and 0.2% of all genes, respectively.

We scanned these genes for YY1 binding sites IPed in cells expressing $YY1^{T372R}$ but not $YY1^{WT}$ that might account for their altered expression. ChIP-seq data from HEK293T cells revealed that the *ADCY1* locus contained 10 instances of the $YY1^{T372R}$ recognition motif residing in a ChIP peak within the gene that was absent with $YY1^{WT}$ (Fig. 3*B*) and 11 instances of the motif in the 4.4 kb surrounding the site of transcription initiation. Similarly, the *CACNA2D2* locus contained a ChIP peak with 16 instances of the $YY1^{T372R}$ motif within intron 3 and additional binding sites near the transcription start site (*SI Appendix*, Fig. S7). Although one cannot project the impact of these observed binding sites in HEK293T cells to effects on transcription in β-cells with certainty, the binding sites for

Cromer et al.

Fig. 3. *ADCY1* is strongly up-regulated and harbors YY1 binding sites upon expression of $YY1^{T372R}$ that are not seen with expression of $YY1^{WT}$. (*A*) Median *ADCY1* expression of each $YY1^{WT}$ (blue) and $YY1^{T372R}$ (red) tumor across all 20 probes. Expression is normalized to the 75th percentile of all probes expressed above background for each sample. Error bars represent SEM. (*B*) ChIP-seq of YY1 in HEK293T cells expressing $YY1^{WT}$ or $YY1^{T372R}$. *ADCY1* shows no binding of $YY1^{WT}$; however, sites bound by $YY1^{T372R}$ replicate in duplicate experiments. (*Inset*) The 400 bp flanking a $YY1^{T372R}$-specific peak within intron 3 are shown. Occurrences of the deduced $YY1^{T372R}$-binding motif, CCATC, are depicted in red. All ChIP input DNA was devoid of visible peaks in this region.

mutant YY1 suggest a mechanism for the increased expression of these genes.

Due to the importance of cAMP and intracellular Ca^{2+} in the regulation of insulin secretion, increased expression of both *ADCY1* and *CACNA2D2* has plausible roles in insulinoma pathogenesis. As noted above, activation of voltage-gated Ca^{2+} channels leads to increased intracellular Ca^{2+}, a sufficient signal for insulin secretion and cell proliferation (37). Increased expression of *CACNA2D2* has previously been shown to increase intracellular Ca^{2+} (38), providing a potential link between increased expression of *CACNA2D2* and increased insulin secretion and/or cell proliferation.

Similarly, cAMP plays an important role in potentiating insulin secretion. *ADCY6* is the most highly expressed adenylyl cyclase isoform in normal β-cells (33). It is activated by the GLP1R subunit Gα and inhibited by intracellular Ca^{2+}. Thus, ADCY6 activation produces a spike in intracellular Ca^{2+} that then inhibits further ADCY6 activity (*SI Appendix*, Fig. S1*B*) (39). In contrast, ADCY1, normally expressed in the CNS, is positively regulated by increased Ca^{2+} and only weakly stimulated by Gα (*SI Appendix*, Fig. S1*C*) (40, 41). Consequently, increased Ca^{2+} levels in cells expressing *ADCY1* are expected to lead to chronic activation of ADCY1 and a sustained increase in cAMP and intracellular Ca^{2+}.
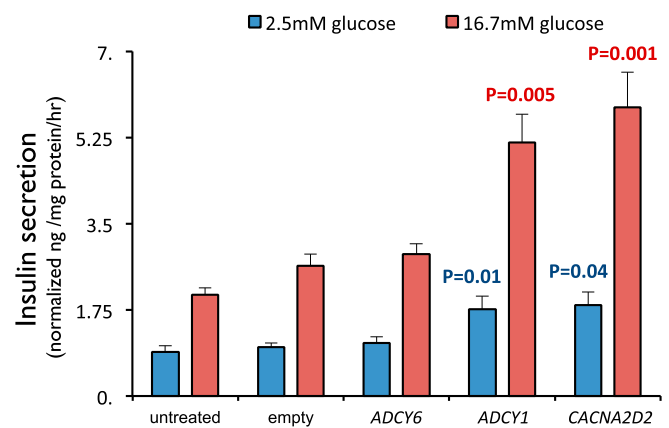
Increased *ADCY1* and *CACNA2D2* Expression Induces Insulin Secretion. To test the effects of increased *ADCY1* and *CACNA2D2* expression on insulin secretion, we compared insulin secretion in the rat INS-1 cell line (a β-cell–derived line that shows insulin

secretion regulated by glucose and membrane potential) (42) following transfection of empty vector, *ADCY6*, *ADCY1*, or *CACNA2D2*. Each transgene (FLAG-tagged *ADCY6*, *ADCY1*, and *CACNA2D2*) produced similar protein levels, which were comparable to endogenous levels of ACTB (*SI Appendix*, Fig. S8). As expected, the empty vector control showed basal insulin secretion in very low glucose that was significantly increased in high glucose (Fig. 4); as expected, high extracellular K^+ also stimulated insulin secretion (*SI Appendix*, Fig. S9). Expression of *ADCY6*, the adenylyl cyclase endogenously expressed in β-cells, produced no significant difference in insulin secretion compared with control in low and high glucose. In contrast, expression of *ADCY1* resulted in approximately twofold higher insulin secretion in both low and high glucose compared with empty vector ($P = 0.01$ and $P = 0.005$, respectively; Fig. 4). Similarly, expression of *CACNA2D2* also resulted in significant increases in insulin secretion, again with approximately twofold increases in insulin secretion at both low and high glucose ($P = 0.04$ and $P = 0.001$, respectively) (Fig. 4). The magnitude of these effects on insulin secretion is similar to those reported for incubation with known insulin secretagogues such as the sulfonylurea tolbutamide and GLP1R agonists (43, 44). Expression of *ADCY1* and *CACNA2D2* together did not produce an additional increase in insulin secretion (*SI Appendix*, Fig. S10).

Discussion

These findings demonstrate that the recurrent $YY1^{T372R}$ mutation in insulinomas changes the DNA binding specificity of this transcription factor, resulting in marked changes in gene expression. Increased expression of two genes not normally regulated by YY1 is shown to contribute to disease pathogenesis. These results provide an example in which alteration of the DNA sequence motif bound by a transcription factor contributes to disease and support neomorphic effects of this recurrent mutation.

Based on known physiology of the regulation of insulin secretion, two genes showing marked increases in expression in $YY1^{T372R}$, *CACNA2D2* and *ADCY1*, were selected as candidates for playing a role in these tumors. Both were found to increase secretion of insulin when expressed in rat INS-1 cells whereas increased expression of the endogenous β-cell adenylyl cyclase *ADCY6* did not. The potential of ectopic expression of the neuronal *ADCY1* to produce a positive feedback system promoting insulin secretion in β-cells is particularly intriguing, with Ca^{2+} entry inducing ADCY1 activity that in turn promotes

Fig. 4. *ADCY1* and *CACNA2D2* cause increased insulin secretion in INS-1 cells. Human *ADCY6*, *ADCY1*, and *CACNA2D2* were transiently expressed and insulin secretion was measured 24 h posttransfection. Compared with empty vector controls, expression of *ADCY1* and *CACNA2D2* significantly increased insulin secretion at both 2.5 and 16.7 mM glucose, whereas expression of *ADCY6* produced no significant change. Comparing to the empty vector control at the appropriate glucose concentration, P values were calculated using Wilcoxon signed-rank test. Error bars represent SEM.

MEDICAL SCIENCES

further Ca^{2+} entry. The ability of *ADCY1* and *CACNA2D2* to significantly increase insulin secretion at both low and high levels of glucose is consistent with the pathology of insulinomas, which can cause life-threatening hypoglycemia by promoting insulin secretion despite low glucose levels (*SI Appendix*, Table S1).

In addition to promoting insulin secretion, the pathways activated by CACNA2D2 and ADCY1 can also increase β-cell proliferation and β-cell mass (11, 12, 45, 46). These *YY1* mutations can thus potentially explain both cardinal features of these tumors. In conjunction with the paucity of other mutations in *YY1*-mutated tumors, it seems likely that these single mutations are sufficient for the development of insulinomas, similar to the role of recurrent *KCNJ5* and *CACNA1D* mutations in adrenal aldosterone-producing adenomas (13, 14).

The relative contributions of *ADCY1* and *CACNA2D2* in the tumors in vivo are uncertain, as we did not find synergistic effects when both were expressed in INS-1 cells (*SI Appendix*, Fig. S10). We also did not observe significant increases in proliferation rates as measured by BrdU incorporation when *ADCY1* and *CACNA2D2* were expressed in INS-1 cells (*SI Appendix*, Fig. S11). This is not surprising, however, given the delicate balance between Ca^{2+} as a proproliferative versus proapoptotic signal (47, 48), the likelihood that levels of expression of *ADCY1* and *CACNA2D2* achieved in native tumors and INS-1 cells are different, and the comparison of short-term effects in an immortal cell line compared with the in vivo situation. Indeed, *KCNJ5* mutations that produce the largest Na^+ conductance are never found in aldosterone-producing adenomas, and are only seen as germ-line mutations without adrenal hyperplasia due to dramatic induction of cell death (49). Nonetheless, the striking induction and ectopic expression of *ADCY1* in these tumors, along with its effect on insulin secretion, support neomorphic effects of the $YY1^{T372R}$ mutation rather than the previously suggested simple increased expression of normal YY1 targets (20).

Although our results clearly demonstrate the ability of ADCY1 and CACNA2D2 to increase insulin secretion in INS-1 cells, we cannot rule out the possibility that other differentially expressed genes play a role in tumorigenesis. Although our expression data indicate that increased *ADCY1* and *CACNA2D2* do not play a role in other insulinomas, the results do not exclude the possibility that alteration of Ca^{2+} signaling or adenylate cyclase pathways via distinct mechanisms may play a role in other insulinomas.

Because the sites bound by $YY1^{T372R}$ are generally not under strong evolutionary constraint (this motif is not specifically bound by any other known factor), we do not expect genes with increased expression in humans to likely show the same alteration in other species. Thus, it is unlikely that expressing $YY1^{T372R}$ in transgenic animals would recapitulate the human findings. Future efforts to determine the consequences of transducing human β-cells with $YY1^{T372R}$ will be of interest.

In addition to $YY1^{T372R}$, exome sequencing identified one tumor with biallelic somatic mutation in *MEN1*. Although MEN1 is a chromatin modifier that plays a role in both familial and sporadic endocrine tumorigenesis, the pathway connecting its mutation to disease pathogenesis remains uncertain. In light of the present findings, it will be of interest to further explore the mechanisms of *MEN1* mutation. Three of the seven tumors sequenced had no clear disease-related mutation, suggesting that additional genes await discovery.

The fact that $YY1^{T372R}$ is frequently found in both benign and malignant insulinomas, but not in malignant pancreatic neuroendocrine tumors that do not secrete insulin (50) or pancreatic ductal adenocarcinomas (51), suggests that this mutation is extremely specific for hormone-producing neoplasms. We expect that $YY1^{T372R}$ is not sufficient for producing malignant tumors without additional mutations. Interestingly, $YY1^{T372R}$ has only been seen in one other context, as a somatic mutation in one aldosterone-producing adenoma (13). Thus, the evidence herein that this mutation acts in β-cell tumors by increasing intracellular Ca^{2+} is consistent with its finding in an aldosteronoma, because

mutations in two other genes that are known to be sufficient for development of these tumors (13, 14) and in two others that are likely sufficient (14, 52) all cause increased intracellular Ca^{2+} (14, 53).

Last, there is considerable interest in the ability to induce proliferation and/or insulin secretion of β-cells in vivo and ex vivo. The genes implicated in insulinomas provide insight into endogenous mechanisms that achieve these effects and suggest that genes and pathways implicated in these tumors may be useful targets for achieving these goals.

Materials and Methods

Insulinoma Samples. Thirty-three benign and 10 malignant pancreatic insulinomas with matched normal blood samples were obtained from patients after surgical removal at the Yale University School of Medicine, University of Connecticut Health Center, and University Hospital, Uppsala. Pancreatic insulinoma was confirmed by fasting hypoglycemia with inappropriately elevated insulin, evidence of a pancreatic tumor by computed tomography scan, MRI scan, and/or endoscopic ultrasound, as well as by a histopathologic diagnosis of pancreatic β-cell insulinoma after surgery (*SI Appendix*, Table S1). Patients with germ-line *MEN1* mutations were excluded. Tumor tissue was dissected by an endocrine pathologist, snap-frozen in optimal cutting temperature (OCT) frozen tissue matrix using liquid nitrogen, and stored at −80 °C until DNA extraction. The research protocol was approved by the Institutional Review Boards of both Yale University and Uppsala University and informed consent was obtained from all participants.

DNA Sequencing and Analysis. Genomic DNA was isolated using standard protocols. Exome capture of seven tumor–normal pairs was performed using NimbleGen Sequence Capture 2.1M as previously described (13). Resulting libraries were sequenced on the Illumina platform using 74-bp paired-end reads. Sequence analysis was performed as previously described (13). Somatic mutations were identified based on a significant difference in read counts between tumor and germ-line DNA as determined using a Fisher's exact test. All somatic mutations were confirmed by Sanger sequencing. Targeted Sanger sequencing of the third zinc finger of YY1 was performed in an additional 36 tumors.

ChIP-Seq. A clone encoding $YY1^{T372R}$ with a C-terminal Myc tag was derived by site-directed mutagenesis of $YY1^{WT}$ in a pCMV6-Entry Vector and verified via Sanger sequencing. HEK293T cells, cultured in DMEM with 10% FBS, were transfected via Lipofectamine 2000 (Life Technologies) within the manufacturer's recommended range of 2.5–5 μg of plasmid encoding $YY1^{WT}$ or $YY1^{T372R}$. Forty-eight hours posttransfection, cells were harvested, lysed, and centrifuged at $800 \times g$ for 5 min; the supernatant was collected and sonicated to produce DNA ranging from 100 to 600 bp. Two hundred micrograms of sheared DNA was used for IP with anti–c-Myc antibody coupled to protein A/G agarose beads (Santa Cruz Biotechnology) as described previously (54). Quantitative (q)PCR of sequences known to be bound by $YY1^{WT}$ confirmed enrichment in samples ChIPed by $YY1^{WT}$ compared with non-ChIPed inputs. The resulting products were sequenced on an Illumina HiSeq, producing a mean of 41 million 74-bp paired-end reads for each of two duplicates for both $YY1^{WT}$ and $YY1^{T372R}$ IPs. Reads were aligned to the hg19 reference genome using Bowtie (54). Reads were trimmed (3 bp from the 5′ end and 15 bp from the 3′ end); >80% of reads of each base showed a Phred quality score >30 (http://www.phrap.com/phred). Enriched regions were identified using MACS (29). Wig format peak signals (http://genome.ucsc.edu/goldenpath/help/wiggle.html) were normalized to reads per million mapped reads using an in-house Perl script. Peaks were input into Galaxy (55) and peaks present in both duplicates were identified; 86% and 58% of peaks replicated in $YY1^{T372R}$ and $YY1^{WT}$ samples, respectively. Replicating peaks showing the greatest enrichment (top 10%) were trimmed to the 20 bp surrounding the MACS-identified summit and used as input for MEME (28). FIMO (30) was then used to scan hg19 for all occurrences of the MEME-identified $YY1^{WT}$ and $YY1^{T372R}$ motifs. The threshold for significant enrichment was the recommended FIMO setting of $P < 10^{-4}$. The resulting motif occurrences were input into Galaxy, and the occurrences of these motifs in random 400-bp genome segments were compared with their prevalence in the top 10% of enriched replicating peaks.

RNA Expression. Five insulinomas with somatic $YY1^{T372R}$ mutation and six with $YY1^{WT}$ underwent RNA expression analysis using the SurePrint G3 Human Exon 4 × 180K Microarray (Agilent Technologies). All probes on the

array were used as input for unsupervised clustering by PCA as implemented by the FactoMineR package in R (http://www.r-project.org). Euclidian distances between all possible $YY1^{WT}$–$YY1^{T372R}$ tumor pairs were compared with distances between all possible $YY1^{WT}$–$YY1^{WT}$ and $YY1^{T372R}$–$YY1^{T372R}$ pairs using a Student's *t* test. Fold change in expression of individual genes between $YY1^{WT}$ and $YY1^{T372R}$ tumors was calculated as the median fold change across all probes for each gene. The significance of changes was calculated from the median log-transformed *P* value across all probes for each gene.

Insulin Secretion Assay. Rat insulinoma cell line INS-1 (42) was cultured in RPMI 1640 with 11 mM glucose and 10% FBS. At 60% confluence, cells were transfected using Lipofectamine with empty vector pCMV6-XL5, human *ADCY6*, human *ADCY1*, or human *CACNA2D2* (cDNAs from OriGene). Twenty-four hours posttransfection, cells were incubated in DMEM with 2.5 mM glucose for 2 h at 37 °C, after which glucose stimulation was performed by incubating cells for 45 min in media containing either 2.5 or 16.7 mM glucose. Secreted insulin levels were measured by ELISA in cell supernatant (ALPCO Diagnostics). Expression of transfected constructs was confirmed via quantitative (q)PCR of RNA. Insulin secretion was measured in each condition for 15–27 wells from three or four independent transfections for each construct. Empty vector controls were performed in all experiments. Wilcoxon signed-rank test was used to test for significant differences in insulin secretion between empty vector control and various treatment groups at the corresponding level of glucose.

1. Batcher E, Madaj P, Gianoukakis AG (2011) Pancreatic neuroendocrine tumors. *Endocr Res* 36(1):35–43.
2. Perry RR, Vinik AI (1995) Clinical review 72: Diagnosis and management of functioning islet cell tumors. *J Clin Endocrinol Metab* 80(8):2273–2278.
3. Li L, Rojas A, Wu J, Jiang C (2004) Disruption of glucose sensing and insulin secretion by ribozyme Kir6.2-gene targeting in insulin-secreting cells. *Endocrinology* 145(9):4408–4414.
4. Miki T, et al. (1998) Defective insulin secretion and enhanced insulin action in KATP channel-deficient mice. *Proc Natl Acad Sci USA* 95(18):10402–10406.
5. Scrocchi LA, Marshall BA, Cook SM, Brubaker PL, Drucker DJ (1998) Identification of glucagon-like peptide 1 (GLP-1) actions essential for glucose homeostasis in mice with disruption of GLP-1 receptor signaling. *Diabetes* 47(4):632–639.
6. Holst JJ (2007) The physiology of glucagon-like peptide 1. *Physiol Rev* 87(4):1409–1439.
7. Doyle ME, Egan JM (2007) Mechanisms of action of glucagon-like peptide 1 in the pancreas. *Pharmacol Ther* 113(3):546–593.
8. Roger B, et al. (2011) Adenylyl cyclase 8 is central to glucagon-like peptide 1 signalling and effects of chronically elevated glucose in rat and human pancreatic beta cells. *Diabetologia* 54(2):390–402.
9. Ozaki N, et al. (2000) cAMP-GEFII is a direct target of cAMP in regulated exocytosis. *Nat Cell Biol* 2(11):805–811.
10. Drucker DJ, Nauck MA (2006) The incretin system: Glucagon-like peptide-1 receptor agonists and dipeptidyl peptidase-4 inhibitors in type 2 diabetes. *Lancet* 368(9548):1696–1705.
11. Sjöholm A (1995) Regulation of insulinoma cell proliferation and insulin accumulation by peptides and second messengers. *Ups J Med Sci* 100(3):201–216.
12. Klinger S, et al. (2008) Increasing GLP-1-induced beta-cell proliferation by silencing the negative regulators of signaling cAMP response element modulator-alpha and DUSP14. *Diabetes* 57(3):584–593.
13. Choi M, et al. (2011) K$^+$ channel mutations in adrenal aldosterone-producing adenomas and hereditary hypertension. *Science* 331(6018):768–772.
14. Scholl UI, et al. (2013) Somatic and germline CACNA1D calcium channel mutations in aldosterone-producing adenomas and primary aldosteronism. *Nat Genet* 45(9):1050–1054.
15. Azizan EA, et al. (2013) Somatic mutations in ATP1A1 and CACNA1D underlie a common subtype of adrenal hypertension. *Nat Genet* 45(9):1055–1060.
16. Goh G, et al. (2014) Recurrent activating mutation in PRKACA in cortisol-producing adrenal tumors. *Nat Genet* 46(6):613–617.
17. Cao Y, et al. (2014) Activating hotspot L205R mutation in PRKACA and adrenal Cushing's syndrome. *Science* 344(6186):913–917.
18. Larsson C, Skogseid B, Oberg K, Nakamura Y, Nordenskjöld M (1988) Multiple endocrine neoplasia type 1 gene maps to chromosome 11 and is lost in insulinoma. *Nature* 332(6159):85–87.
19. Zhuang Z, et al. (1997) Somatic mutations of the MEN1 tumor suppressor gene in sporadic gastrinomas and insulinomas. *Cancer Res* 57(21):4682–4686.
20. Cao Y, et al. (2013) Whole exome sequencing of insulinoma reveals recurrent T372R mutations in YY1. *Nat Commun* 4:2810.
21. Shi Y, Lee JS, Galvin KM (1997) Everything you have ever wanted to know about Yin Yang 1...... *Biochim Biophys Acta* 1332(2):F49–F66.
22. Thorvaldsen JL, Weaver JR, Bartolomei MS (2011) A YY1 bridge for X inactivation. *Cell* 146(1):11–13.
23. Jeon Y, Lee JT (2011) YY1 tethers Xist RNA to the inactive X nucleation center. *Cell* 146(1):119–133.
24. Chandrasekharappa SC, et al. (1997) Positional cloning of the gene for multiple endocrine neoplasia-type 1. *Science* 276(5311):404–407.
25. Wu G, et al.; St. Jude Children's Research Hospital–Washington University Pediatric Cancer Genome Project (2012) Somatic histone H3 alterations in pediatric diffuse intrinsic pontine gliomas and non-brainstem glioblastomas. *Nat Genet* 44(3):251–253.
26. Kim JD, Kim J (2009) YY1's longer DNA-binding motifs. *Genomics* 93(2):152–158.
27. Houbaviy HB, Usheva A, Shenk T, Burley SK (1996) Cocrystal structure of YY1 bound to the adeno-associated virus P5 initiator. *Proc Natl Acad Sci USA* 93(24):13577–13582.
28. Bailey TL, Williams N, Misleh C, Li WW (2006) MEME: Discovering and analyzing DNA and protein sequence motifs. *Nucleic Acids Res* 34(Web Server issue):W369–W373.
29. Zhang Y, et al. (2008) Model-based analysis of ChIP-Seq (MACS). *Genome Biol* 9(9):R137.
30. Grant CE, Bailey TL, Noble WS (2011) FIMO: Scanning for occurrences of a given motif. *Bioinformatics* 27(7):1017–1018.
31. Xi H, et al. (2007) Analysis of overrepresented motifs in human core promoters reveals dual regulatory roles of YY1. *Genome Res* 17(6):798–806.
32. Pagliarini DJ, et al. (2008) A mitochondrial protein compendium elucidates complex I disease biology. *Cell* 134(1):112–123.
33. Wang H, Ferguson GD, Pineda VV, Cundiff PE, Storm DR (2004) Overexpression of type-1 adenylyl cyclase in mouse forebrain enhances recognition memory and LTP. *Nat Neurosci* 7(6):635–642.
34. Leech CA, Castonguay MA, Habener JF (1999) Expression of adenylyl cyclase subtypes in pancreatic beta-cells. *Biochem Biophys Res Commun* 254(3):703–706.
35. Kutlu B, et al. (2009) Detailed transcriptome atlas of the pancreatic beta cell. *BMC Med Genomics* 2:3.
36. Delmeire D, et al. (2003) Type VIII adenylyl cyclase in rat beta cells: Coincidence signal detector/generator for glucose and GLP-1. *Diabetologia* 46(10):1383–1393.
37. Nguidjoe E, et al. (2011) Heterozygous inactivation of the Na/Ca exchanger increases glucose-induced insulin release, β-cell proliferation, and mass. *Diabetes* 60(8):2076–2085.
38. Carboni GL, et al. (2003) CACNA2D2-mediated apoptosis in NSCLC cells is associated with alterations of the intracellular calcium signaling and disruption of mitochondria membrane integrity. *Oncogene* 22(4):615–626.
39. Hanoune J, Defer N (2001) Regulation and role of adenylyl cyclase isoforms. *Annu Rev Pharmacol Toxicol* 41:145–174.
40. Cooper DM, Mons N, Karpen JW (1995) Adenylyl cyclases and the interaction between calcium and cAMP signalling. *Nature* 374(6521):421–424.
41. Kitaguchi T, Oya M, Wada Y, Tsuboi T, Miyawaki A (2013) Extracellular calcium influx activates adenylate cyclase 1 and potentiates insulin secretion in MIN6 cells. *Biochem J* 450(2):365–373.
42. Asfari M, et al. (1992) Establishment of 2-mercaptoethanol-dependent differentiated insulin-secreting cell lines. *Endocrinology* 130(1):167–178.
43. Dames P, et al. (2012) Suppression of the nuclear factor Eny2 increases insulin secretion in poorly functioning INS-1E insulinoma cells. *Exp Diabetes Res* 2012:460869.
44. Popiela H, Moore W (1991) Tolbutamide stimulates proliferation of pancreatic beta cells in culture. *Pancreas* 6(4):464–469.
45. Hussain MA, et al. (2006) Increased pancreatic beta-cell proliferation mediated by CREB binding protein gene activation. *Mol Cell Biol* 26(20):7747–7759.
46. Hui H, Nourparvar A, Zhao X, Perfetti R (2003) Glucagon-like peptide-1 inhibits apoptosis of insulin-secreting cells via a cyclic 5′-adenosine monophosphate-dependent protein kinase A- and a phosphatidylinositol 3-kinase-dependent pathway. *Endocrinology* 144(4):1444–1455.
47. Munaron L, Antoniotti S, Lovisolo D (2004) Intracellular calcium signals and control of cell proliferation: How many mechanisms? *J Cell Mol Med* 8(2):161–168.
48. Olofsson MH, Havelka AM, Brnjic S, Shoshan MC, Linder S (2008) Charting calcium-regulated apoptosis pathways using chemical biology: Role of calmodulin kinase II. *BMC Chem Biol* 8:2.
49. Scholl UI, et al. (2012) Hypertension with or without adrenal hyperplasia due to different inherited mutations in the potassium channel KCNJ5. *Proc Natl Acad Sci USA* 109(7):2533–2538.
50. Jones S, et al. (2008) Core signaling pathways in human pancreatic cancers revealed by global genomic analyses. *Science* 321(5897):1801–1806.
51. Jiao Y, et al. (2011) DAXX/ATRX, MEN1, and mTOR pathway genes are frequently altered in pancreatic neuroendocrine tumors. *Science* 331(6021):1199–1203.
52. Beuschlein F, et al. (2013) Somatic mutations in ATP1A1 and ATP2B3 lead to aldosterone-producing adenomas and secondary hypertension. *Nat Genet* 45(4):440–444.
53. Reddy TE, et al. (2009) Genomic determination of the glucocorticoid response reveals unexpected mechanisms of gene regulation. *Genome Res* 19(12):2163–2171.
54. Langmead B, Trapnell C, Pop M, Salzberg SL (2009) Ultrafast and memory-efficient alignment of short DNA sequences to the human genome. *Genome Biol* 10(3):R25.
55. Giardine B, et al. (2005) Galaxy: A platform for interactive large-scale genome analysis. *Genome Res* 15(10):1451–1455.

MEDICAL SCIENCES